

# MHD Boundary Layer Flow of a Nanofluid Past a Wedge Shaped Wick in Heat Pipe

Ziya Uddin

**Abstract**—This paper deals with the theoretical and numerical investigation of magneto hydrodynamic boundary layer flow of a nanofluid past a wedge shaped wick in heat pipe used for the cooling of electronic components and different type of machines. To incorporate the effect of nanoparticle diameter, concentration of nanoparticles in the pure fluid, nanothermal layer formed around the nanoparticle and Brownian motion of nanoparticles etc., appropriate models are used for the effective thermal and physical properties of nanofluids. To model the rotation of nanoparticles inside the base fluid, microfluidics theory is used. In this investigation ethylene glycol (EG) based nanofluids, are taken into account. The non-linear equations governing the flow and heat transfer are solved by using a very effective particle swarm optimization technique along with Runge-Kutta method. The values of heat transfer coefficient are found for different parameters involved in the formulation viz. nanoparticle concentration, nanoparticle size, magnetic field and wedge angle etc. It is found that, the wedge angle, presence of magnetic field, nanoparticle size and nanoparticle concentration etc. have prominent effects on fluid flow and heat transfer characteristics for the considered configuration.

**Keywords**—Heat transfer, Heat pipe, numerical modeling, nanofluid applications, particle swarm optimization, wedge shaped wick.

## I. INTRODUCTION

A detailed study about the heat pipes can be found in [1]. The rate of heat transfer depends upon the design of the wick structure in heat pipe and the working fluid inside the heat pipe having high value of thermal conductivity. The traditional fluids like water, ethylene glycol or oil etc. have low values of thermal conductivity. On the other hand, the metals and their oxide have high thermal conductivities compared to these fluids. Choi et al. [2] proposed that the uniform dispersion of small concentration of nano-sized metal/metal oxides particles into a fluid enhances the thermal conductivity of the base fluid, and such fluids were termed as nanofluids. Taking this concept in mind various researchers have worked on the experimental and theoretical studies on thermo physical properties of nanofluids. An extensive review of thermal properties of nanofluids can be found in [3]. Literature survey reveals that the thermal conductivity of nanofluids depends upon various factors, such as nanoparticle size, nanoparticle concentration in the base fluid, nanoparticle material, base fluid properties, Brownian motion of the nanoparticles in base fluid, nanoparticle shape, nanoparticle base fluid interfacial layer, and particle clustering etc. Wang et

al. [4] found that the insertion of nanoparticle increases the viscosity of the fluid. Yu et al. [5] investigated the role of interfacial layers in the enhanced thermal conductivity of nanofluids using a renovated Maxwell model. Various theoretical studies have been done to model the thermal conductivity and viscosity of nanofluids, but these modeled mathematical expressions do not satisfy the experimental data up to a satisfying range. Corcione [6] analyzed the experimental data of thermal conductivity and viscosity of nanofluids, which were obtained by various researchers for different types of nanoparticles, dispersed in different base fluids, and found an empirical correlating equation for the prediction of effective thermal conductivity and dynamic viscosity of nanofluids. Invention of nanofluids attracted various researchers towards the applications of nanofluids in industry. Uddin et al. [7] studied the natural convection heat transfer of nanofluids along a vertical plate embedded in porous medium and found that nanofluids help in the enhancement of heat transfer rate. Mohsen et al. [8] found the numerical results for the MHD nanofluid flow and heat transfer considering viscous dissipation.

As, the nanofluids have high thermal conductivity as compared to the common fluids. Therefore, nanofluid is a good option to enhance the heat transfer rate in heat pipe. A detailed description about the use of nanofluids in different heat pipes can be found in [9] and [10]. Flow around the wedge shaped bodies is also of great industrial importance; therefore, various studies have been done on this topic. Uddin et al. [11] proved that the heat transfer rate for the flow around a wedge shaped body is high as compared to the flow around a horizontal plate under the same flow conditions. Authors also, showed that the increase in wedge angle increases the heat transfer rate.

From the literature survey, it is observed that, the heat transfer depends upon the shape of the body and the nature of the fluid. In the author's knowledge no work has been done earlier for the flow of a nanofluid past a wedge shaped wick in presence of magnetic field. Therefore, the scope of the current research is to implement the appropriate models for the nanofluid thermos physical properties, and to analyze the effect of nanofluids on heat transfer enhancement using the nanofluids inside the heat pipe with wedge shaped wick structure.

## II. MATHEMATICAL FORMULATION

In the present mathematical model, steady viscous, incompressible, nanofluid flowing past a wedge shaped wick in heat pipe is considered. The physical model and coordinate

Z. U. is with the BML Munjal University, SoET, 67 Milestone, NH-8, Gurgaon, India, 123413(phone: +918295200293; e-mail: ziya.uddin@bml.edu.in).

system of the flow past wedge shaped wick is shown in Fig. 1. A rectangular coordinate system is used for the formulation, in which  $x$ ,  $y$  and  $z$  are the distances measured along the wedge, normal to the surface of the wedge and along the leading edge of the wedge respectively. Magnetic field  $B(x)$  acts along  $y$ -axis. It is considered that the nanoparticles inside the pure fluid have rotations as well as Brownian motion.

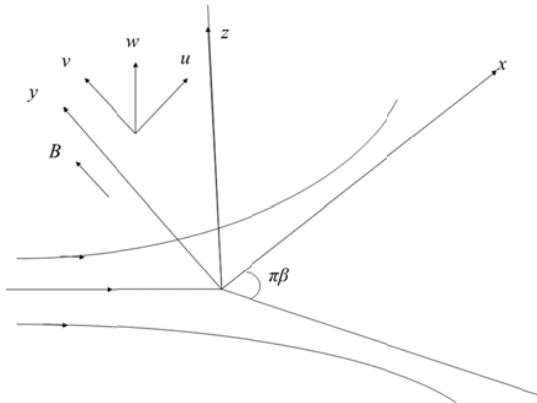


Fig. 1 Physical Model and coordinate system

Considering these assumptions and following [11], the equations for the liquid flow and heat transfer in non-dimensional form are:

$$(1+K)f'''' + ff'' + \left(\frac{2m}{m+1}\right)(1-f'^2) + Kh' + M(1-f') = 0 \quad (1)$$

$$(1+K)g'' + g'f' - \left(\frac{2m}{m+1}\right)gf' - Mg = 0 \quad (2)$$

$$\left(1 + \frac{K}{2}\right)h'' - \left[\left(\frac{3m-1}{m+1}\right)hf' - fh'\right] - \frac{2KI}{m+1}(2h + f''') = 0 \quad (3)$$

$$\frac{1}{Pr}\theta'' + (m+1)f\theta' + (m-1)g\theta' = 0 \quad (4)$$

where, (') represents the derivative with respect to  $\eta$ ,  $\psi$  is stream function. Therefore,  $u = \frac{\partial \psi}{\partial y}$  and  $v = -\frac{\partial \psi}{\partial x}$ .

The similarity variables used in above equations are:

$$\begin{aligned} \psi &= f(\eta) \left( \frac{2\nu_f x U}{m+1} \right)^{1/2} N = U h(\eta) \left( \frac{(m+1)U}{2\nu_f x} \right)^{1/2} \eta = \left[ \frac{(m+1)U}{2\nu_f x} \right]^{1/2} y \\ \theta(\eta) &= \frac{k_f(T - T_\infty)}{q_\infty} \left( \frac{(m+1)U}{2\nu_f x} \right)^{1/2} M = \frac{2\sigma_{nf} B^2}{a\rho_{nf}(m+1)}, \quad w = U g(\eta), \\ Pr &= \frac{\mu_{nf} C_p}{k_{nf}} B = \frac{\nu_{nf}^2 Re}{JU^2} \end{aligned}$$

It is known that  $\gamma_{nf} = \mu_{nf}(1+K/2)j$ , where  $K = \kappa/\mu$  is dimensionless viscosity ratio and is called as material parameter.

Initial and Boundary conditions in non-dimensional form

are:

$$\begin{aligned} f(0) &= 0, \quad f'(0) = 0, \quad g(0) = 0, \quad \theta'(0) = -1, \quad h(0) = -f''(0)/2, \\ f'(\infty) &\rightarrow 1, \quad g(\infty) \rightarrow 0, \quad h(\infty) \rightarrow 0, \quad \theta(\infty) \rightarrow 0 \end{aligned} \quad (5)$$

Local skin friction coefficients ( $C_{fx}$  and  $C_{fz}$ ) and local Nusselt number ( $Nu$ ) in non-dimensional form are defined as:

$$C_{fx} = \sqrt{\frac{2(m+1)}{Re}} \left(1 + \frac{K}{2}\right) f''(0) \quad \text{and} \quad Nu = \sqrt{\frac{(m+1)Re}{2}} \frac{1}{\theta(0)}$$

respectively.

Following [7] the nanofluid properties are

$$\begin{aligned} \rho_{nf} &= \phi \rho_p + (1-\phi) \rho_f \\ (\rho C_p)_{nf} &= \phi(\rho C_p)_p + (1-\phi)(\rho C_p)_f \end{aligned}$$

The viscosity of nanofluid is given by:

$$\begin{aligned} \mu_{nf} &= \frac{\mu_f}{1 - 34.87(d_p/d_f)^{0.3} \phi^{1.03}} \\ d_f &= 0.1 \left[ \frac{6M}{N\pi\rho_{fo}} \right]^{1/3} \end{aligned}$$

Here  $d_f$  is the diameter of base fluid molecule,  $M$  is the molecular weight of the base fluid,  $N$  is the Avogadro number, and  $\rho_{fo}$  is the mass density of the base fluid calculated at the reference temperature (293K).

Following [9], the thermal conductivity of nanofluid is given by:

$$\begin{aligned} k_{nf} &= \left[ \frac{k_{pe} + 2k_b + 2(k_{pe} - k_b)(1-\beta)^3 \phi}{k_{pe} + 2k_b - 2(k_{pe} - k_b)(1+\beta)^3 \phi} \right] k_b \\ k_{pe} &= \delta \left[ \frac{2(1-\delta) + (1-\beta)^3(1+2\delta)}{-(1-\delta) + (1+\beta)^3(1+2\delta)} \right] k_b \\ \delta &= \frac{k_{layer}}{k_p} \\ \beta &= \frac{h}{r_p} \end{aligned}$$

Here  $k_{layer}$  is the thermal conductivity of the nanolayer formed by the base fluid particles around nanoparticle in the nanofluid and  $h$  is the thickness of this thermal layer. Following [5],  $k_{layer} = 100k_f$  and  $h = 2 \text{ nm}$  have been considered during computations.

The electrical conductivity for the nanofluid is taken from [8]

$$\sigma_{nf} = \left[ 1 + \frac{3 \left( \frac{\sigma_p}{\sigma_f} - 1 \right) \phi}{\left( \frac{\sigma_p}{\sigma_f} + 2 \right) - \left( \frac{\sigma_p}{\sigma_f} - 1 \right) \phi} \right] \sigma_f$$

### III. METHOD OF SOLUTION

Taking the nanofluid properties into account, the non-linear ordinary differential equations (1)–(4) subjected to the initial and boundary conditions (5) have been solved by using Runge-Kutta Fehlberg integration method along with Particle swarm optimization (PSO) [12]. This method is based on the discretization of the problem domain and the calculation of unknown initial conditions using PSO. The domain of the problem is discretized and the boundary conditions for  $\eta = \infty$  are replaced by  $f'(\eta_{\max}) = 1$ ,  $g(\eta_{\max}) = 1$ ,  $h(\eta_{\max}) = 1$  and  $\theta(\eta_{\max}) = 0$ , where  $\eta_{\max}$  is a sufficiently large value of  $\eta$  (corresponding to step size) at which the boundary conditions (5) for  $f(\eta)$  is satisfied. In the present work we have set  $\eta_{\max} = 3$  taking into account the consistency and stability criteria. To find the solution of these coupled equations we employed the numerical integration technique based on PSO where the ending boundary conditions are utilized to produce unknown initial conditions under the convergence criteria of  $\sqrt{(1 - f'(\infty))^2 + g(\infty)^2 + h(\infty)^2 + \theta(\infty)^2} \leq 10^{-8}$ .

### IV. RESULTS AND DISCUSSION

The computations have been carried out for the CuO+EG (ethylene glycol) nanofluid under different conditions. The thermo-physical properties of pure CuO and pure EG at reference temperature (293K) are given in Table I. The effects of various parameters involved in the problem on the velocity profiles and temperature distributions are found and represented in Figs. 2–9. The values of heat transfer coefficient and skin friction coefficient have also been calculated, and presented in Table II.

TABLE I  
THERMAL PROPERTIES OF CUO AND EG AT REFERENCE TEMPERATURE (293K)

	CuO	EG
$\rho$	6500	1105.2
$C_p$	540	2452.9
$k$	18	0.2546
$\mu$	-	0.0118
$M$	-	0.06207
$\rho_{fo}$	-	1112.1
$\rho_v$	-	9.2

The effect of nanoparticle concentration on the velocity profiles and temperature distribution is shown in Figs. 2–4. Fig. 2 depicts that the temperature as well as thermal boundary layer thickness decreases with the increase in value of nanoparticle concentration in pure fluid. Therefore, the local Nusselt number increases with the increasing value of concentration. The variation of Nusselt number is shown in Table II. With the increase in nanoparticle concentration, horizontal velocity increases and after a fixed distance away from the surface it decreases, while the transverse velocity shows a uniform increasing pattern with the increase in the

value of concentration as depicted in Figs. 3 and 4. It is also clear from the figures that the velocity gradients near the surface increase, and hence produce an increase in skin friction coefficients. Thus nanofluids show the increase in local skin drag as compared to pure fluids. The numerical values of skin friction coefficients for various values of concentration are given in Table II.

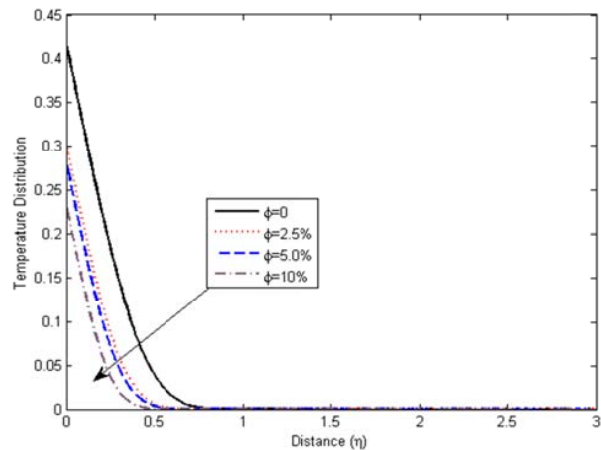


Fig. 2 Temperature distribution Vs.  $\phi$  for  $M=1$ ,  $m=1/3$ ,  $dp=10$

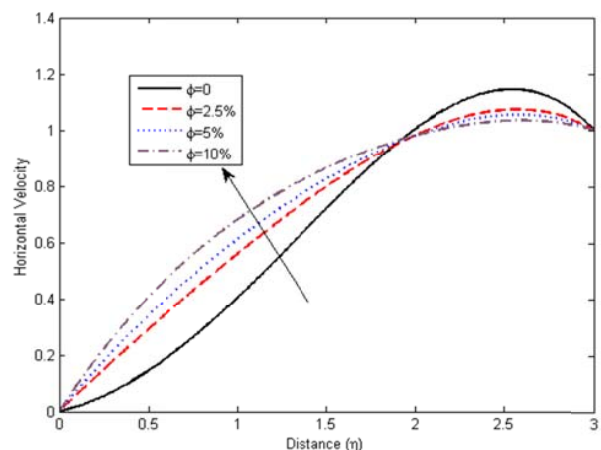


Fig. 3 Horizontal velocity Vs.  $\phi$  for  $M=1$ ,  $m=1/3$ ,  $dp=10$

Fig. 5 depicts that the absolute value of angular velocity near the surface increases with the increase in the value of concentration, and as we move away from the wedge this value decreases. These changes result in a decrease in rotation of the nanoparticle near the surface and hence increase the wall couple stress. Thus the increase in nanoparticle concentration accelerates the particle rotation near the surface.

Figs. 6–9 depict the effect of nanoparticle size on velocities and temperature distribution. Fig. 6 depicts that with the increase in nanoparticle diameter the thermal boundary layer thickness increases, which results in the decrease in heat transfer rate. This result can also be confirmed in Table II. From Table II it is clear that with the increase in nanoparticle diameter, the value of Nusselt number, i.e. heat transfer rate decreases.

From Fig. 7, it is depicted that, the horizontal velocity increases slightly with the increase in nanoparticle diameter. This increases the velocity gradient near the wall and results the increase in local skin friction coefficient. The values of skin friction coefficients for various values of nanoparticle diameter are given in Table II. The effect of nanoparticle diameter on transverse component of velocity is shown in Fig. 8. This figure shows that the increase in nanoparticle diameter decreases the transverse velocity component. This causes the increase in transverse velocity gradient, thus increases the local skin friction coefficient. This result is also verified by the calculated values given in Table II.

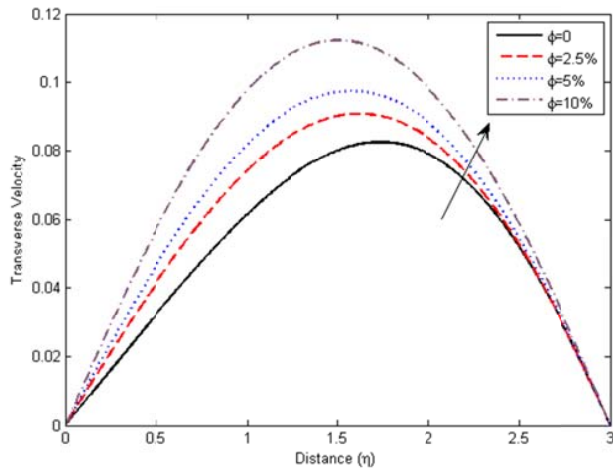


Fig. 4 Transverse velocity Vs.  $\phi$  for  $M=1$ ,  $m=1/3$ ,  $dp=10$

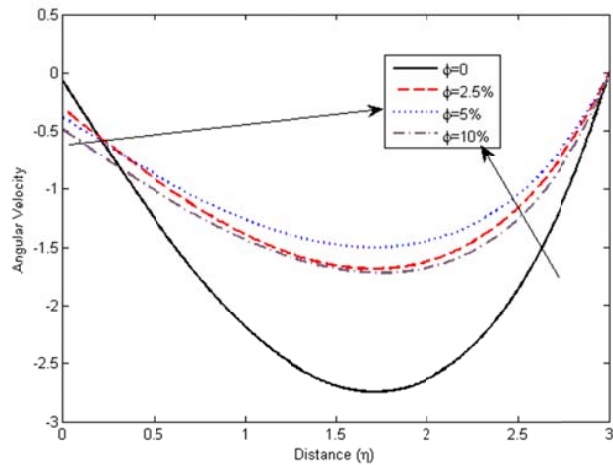


Fig. 5 Angular velocity Vs.  $\phi$  for  $M=1$ ,  $m=1/3$ ,  $dp=10$

From Fig. 9 it is observed that the magnitude of angular velocity decreases with the increase in nanoparticle diameter, this causes the decrease in angular velocity gradient near the wall, and results in the decreased wall couple stress.

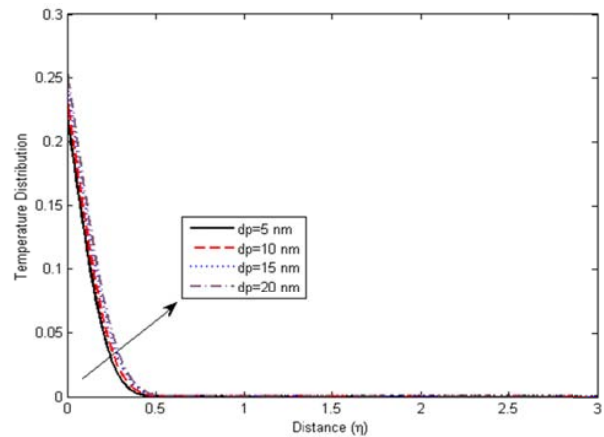


Fig. 6 Temperature distribution Vs.  $dp$  for  $M=1$ ,  $m=1/3$  and  $\phi=0.1$

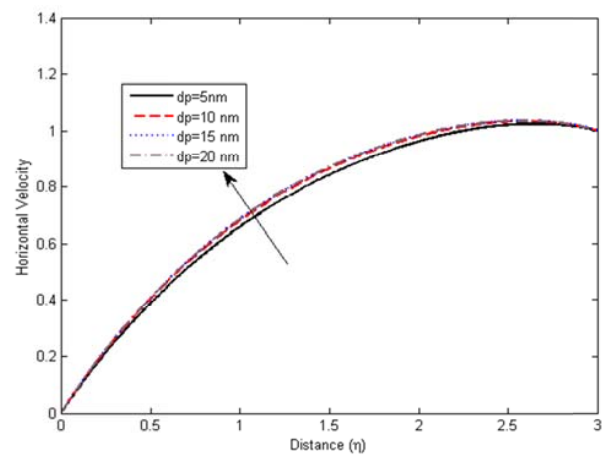


Fig. 7 Horizontal Velocity Vs.  $dp$  for  $M=1$ ,  $m=1/3$  and  $\phi=0.1$

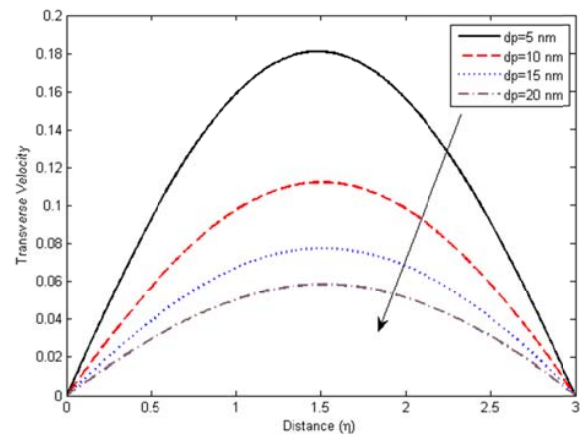
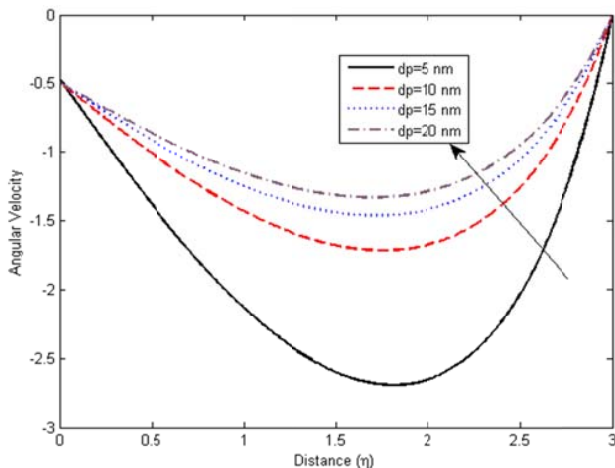


Fig. 8 Transverse Velocity Vs.  $dp$  for  $M=1$ ,  $m=1/3$  and  $\phi=0.1$

Fig. 9 Angular Velocity Vs. dp for  $M=1$ ,  $m=1/3$  and  $\phi=0.1$ TABLE II  
VALUES OF NUSSELT NUMBER AND SKIN FRICTION COEFFICIENT

M	m	Dp	$\Phi$	$Nu.Re^{1/2}$	$C_f.Re^{1/2}$
0	1/3	10	10%	3.2144332	1.4005733
1	1/3	10	10%	3.4979761	1.8532349
2	1/3	10	10%	3.6909557	2.2173265
1	0	10	10%	3.0413140	1.4889499
1	1/4	10	10%	3.4492194	1.8579589
1	1/3	5	10%	3.7094226	1.6460079
1	1/3	15	10%	3.31396887	1.9310621
1	1/3	20	10%	3.19684978	1.9708979
1	1/3	10	0	1.95387684	0.3781645
1	1/3	10	2.5%	2.69054569	1.4271409
1	1/3	10	5%	2.88699335	1.6720255

TABLE III  
NOMENCLATURE

Symbol	Quantity	Unit
T	Temperature	(°C)
k	thermal conductivity	(W m <sup>-1</sup> K <sup>-1</sup> )
u,v,w	Velocity	(m s <sup>-1</sup> )
M	Molecular mass of pure fluid	(kg)
Cp	specific heat	(J kg <sup>-1</sup> K <sup>-1</sup> )
N	Avogadro's number (6.0223x10+23)	
x,y,z	coordinate axes	
<b>Greek symbols</b>		
$\rho$	Density	(kg m <sup>-3</sup> )
$\sigma$	Electrical conductivity	(Ohm-m)
$\mu$	Viscosity	(Pa s)
m	Angle	(degree)
$\phi$	nanoparticle concentration	
$\beta$	ratio of nanolayer thickness to nanoparticle radius	
$\delta$	ratio of nanolayer thermal conductivity to nanoparticle thermal conductivity	
<b>Subscripts</b>		
f	pure fluid (liquid)	
nf	Nanofluid	
p	Nanoparticle	

The effect of wedge angle and magnetic field on heat transfer and skin friction coefficient can be seen from Table II. From the table it is observed that for different values of magnetic field parameter  $M$ , keeping all the factors as constant, the Nusselt number as well as skin friction coefficient increase. Therefore, use of magnetic field is a good option to enhance the heat transfer rate. Similarly, with increasing values of wedge angle parameter, the heat transfer rate and skin friction increase.

## V.CONCLUSIONS

From this research it is concluded that the heat transfer rate can be enhanced by increasing the nanoparticle concentration in the pure base fluid, and use of small sized nanoparticles helps more in this enhancement. The wedge angle also plays an important role in the heat transfer rate. From the current study it is also concluded that the for large wedge angle, the heat transfer is more. Similarly, the heat transfer can be enhanced by keeping the wedge in a strong magnetic field.

## REFERENCES

- [1] A. Faghri, Heat Pipe Science and Technology, Taylor & Francis, 1994.
- [2] S. Choi, J. A. Eastman, "Enhancing thermal conductivity of fluids with nanoparticles. In Developments and Applications of Non-Newtonian Flows," Edited by Siginer DA, Wang HP. New York: American Society of Mechanical Engineers, 1995, pp. 99–105.
- [3] X-Q Wang, A. S. Majumdar, "Heat transfer characteristics of nanofluids: a review," Int J Thermal Sci, 2007, vol. 46, pp. 1–19.
- [4] X-Q Wang, A. S. Majumdar, "A review on nanofluids - part I: theoretical and numerical investigations," Braz J Chem Eng, 2008, vol. 25(4), pp. 613–630.
- [5] W. Yu and S. U. S. Choi, "The role of interfacial layers in the enhanced thermal conductivity of nanofluids: A renovated Maxwell model," J Nanoparticle research, 2003, vol. 5, pp. 167–171.
- [6] M. Corcione, "Empirical correlating equations for predicting the effective thermal conductivity and dynamic viscosity of nanofluids," Energy Convers Manage, 2011, vol. 52, pp. 789–793.
- [7] Z. Uddin and S. Harmand, "Natural convection heat transfer of nanofluids along a vertical plate embedded in porous medium," Nanoscale Research Letters, 2013, 8:64.
- [8] Mohsen Sheikholeslami, Shirley Abelman and Davood Domiri Ganji, "Numerical simulation of MHD nanofluid flow and heat transfer considering viscous dissipation," International Journal of Heat and Mass Transfer, 2014, vol. 79, pp. 212–222.
- [9] M. Shafahi, V. Bianco, K. Vafai, O. Manca, "An investigation of the thermal performance of cylindrical heat pipes using nanofluids," Int. J. Heat Mass Transfer, 2010, vol. 53, pp. 376–383.
- [10] Liu Zhen-Hua, Li, Yuan-Yang, "A new frontier of nanofluid research – Application of nanofluids in heat pipes," International Journal of Heat and Mass Transfer, 2012, Vol.55(23-24), pp.6786-6797.
- [11] Z. Uddin and M. Kumar, "Hall and ion-slip effect on MHD boundary layer flow of a micro polar fluid past a wedge," Scientia Iranica B, 2013, vol. 20 (3), pp. 467–476.
- [12] R. Poli, J. Kennedy, T. Blackwell, Particle swarm optimization An overview, Swarm Intell, DOI 10.1007/s11721-007-0002-0, (2007).